Experimental and Theoretical Study of Selectivity in Mechanochemical Cocrystallization of Nicotinamide with Anthranilic and Salicylic Acid

Published as part of a Crystal Growth and Design virtual special issue Honoring Prof. William Jones and His Contributions to Organic Solid-State Chemistry

Stipe Lukin,[†] Ivor Lončarić,[†] Martina Tireli,[†] Tomislav Stolar,[†] Maria V. Blanco,[‡] Predrag Lazić,[†] Krunoslav Užarević,[†] and Ivan Halasz*[,†]

[†]Ruđer Bošković Institute, Bijenička c. 54, 10000 Zagreb, Croatia

[‡]ESRF - the European Synchrotron, 71 Avenue des Martyrs, 38000 Grenoble, France

Supporting Information

ABSTRACT: Selectivity in mechanochemical cocrystal formation between nicotinamide and anthranilic acid or salicylic acid was studied using tandem in situ reaction monitoring by powder X-ray diffraction (PXRD) and Raman spectroscopy. Selectivity was probed by offering a competing cocrystal coformer to a previously prepared cocrystal or under competitive reaction conditions where all cocrystal coformers, in different stoichiometric ratios, were introduced together in the starting reaction mixture. Reaction paths were dependent on the starting mixture composition, and we find that the formation of intermediates and the final product can be predicted from solid-state ab initio calculations of relative energies of possible reaction mixtures. In some cases, quantitative assessment revealed different reaction profiles derived from PXRD and Raman monitoring, directly indicating, for the first time, different mechanochemical reactivity on the molecular and the bulk crystalline level of the reaction mixture.

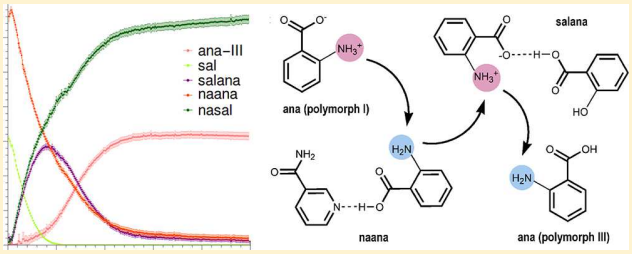

INTRODUCTION

Mechanochemical reactions are becoming increasingly attractive since they offer a means to perform selective chemical synthesis with excellent atom- and energy-economy and with little or, in some cases, no waste generation.[1−3] Being previously limited largely to processing of minerals, metals, alloys, and inorganic materials,[4] chemical transformations achievable by using mechanochemistry now encompass almost every aspect of chemical synthesis, including synthesis of organic,[5−8] organometallic,[9−11] metal−organic compounds[12−14] as well as multicomponent solids such as cocrystals[15,16] and the preparation of nanoparticles,[17] molecular nanostructures,[18] pharmaceuticals,[19] advanced peptide synthesis,[20,21] supramolecular recognition,[22] and recently, enzymatic catalysis.[23,24] The widespread use of mechanochemistry has been since recently accompanied by methodology to probe the course and mechanisms of milling reactions by real-time in situ monitoring techniques based on X-ray diffraction,[25,26] Raman spectroscopy,[9,27] or their simultaneous use in tandem.[28,29]

These techniques have revealed surprisingly fast mechanochemical reactions and metastable and short-lived intermediates, indicating that mechanochemical reactions may bear a strong resemblance to solution chemistry, despite them being conducted in the solid state. Moreover, we hypothesize that many principles derived for solution reactions may also be valid for mechanochemical reactions. In principle, we believe that a surface of potential energy could be constructed where each stable solid phase would lie in its minimum and where energy barriers could be identified for their potential transformations.[30−32] So far, such an energy landscape is evidenced by the observation of the Ostwald's rule of stages,[29,33] the equilibration of solids,[34−36] and a stronger than expected influence of temperature on mechanochemical reactions.[37] Also, while the catalytic effect of liquid additives is well-known,[38,39] direct observation of lowering of an energy barrier and hence reaction acceleration by different liquid additives in a liquid-assisted grinding (LAG) reaction was recently observed.[40] In creating parallels with solution reactions, one also needs to consider solvation of solid particles,[41] which seems to have enabled control over selective preparation of three polymorphs of nicotinamide/benzoic acid cocrystals.[29]

Specific energy relations between solids in an energy landscape would need to result in selectivity in mechanochem-

Received: October 30, 2017
Revised: January 5, 2018

ical reactions. Indeed, in a pioneering study, Etter has shown specific pairing of nucleobases in a grinding reaction in the presence of a competing nucleobase.[42] Caira and co-workers have also shown selective cocrystal preparation starting from a mixture of cocrystal coformers,[43] but they have taken their study a step further in showing that an already formed cocrystal will react if a more selective coformer is offered. In a more recent example, we have shown strong selectivity in supramolecular anion binding with the ability of a host molecule to discriminate even among six dicarboxylic acids.[22] Abourahma and co-workers have studied the robustness of a particular theophylline cocrystal while grinding with other potential coformers and offered a qualitative interpretation of coformer replacements based on hydrogen bonding preferences.[44] Emmerling and co-workers have described a selectivity study between several active pharmaceutical ingredients and anthranilic acid as a cocrystal coformer and suggested that energetic and kinetic factors may need to be taken into account as well.[45]

Herein, we describe selectivity in mechanochemical cocrystal formation between nicotinamide (na) and two benzenecarboxylic acids differing in the functionality on the ortho position: anthranilic acid (ana) and salicylic acid (sal) (Figure 1). Via

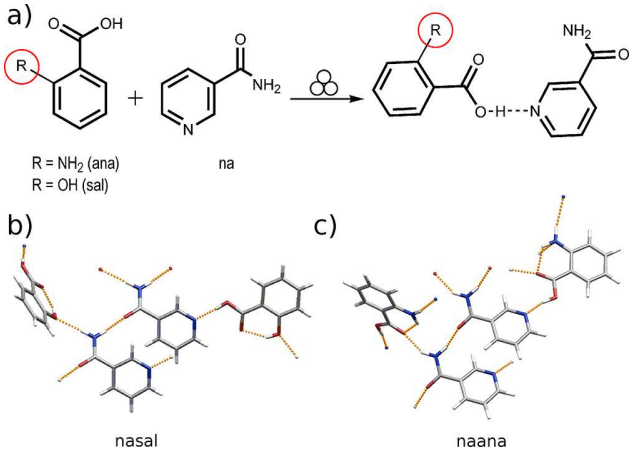

Figure 1. (a) Mechanochemical preparation of cocrystals of na with sal and ana. Hydrogen bonding in the (b) crystal structure of the nasal cocrystal[46] and (c) crystal structure of the naana cocrystal.

quantitative assessment by tandem in situ powder X-ray diffraction and Raman monitoring,[29] we have observed varied and intricate reaction paths in competitive cocrystal formation and cocrystal replacement reactions, involving formation of metastable intermediates and multistep solid-state proton transfer. Accompanied by theoretical calculations of stabilities of participating solid phases, we find that the observed selectivity can be readily predicted from relative stabilities of cocrystals and coformers, while the reaction mechanisms may nevertheless involve various, less stable intermediate phases. In the course of this study we have solved, from powder diffraction data, the crystal structure of the nicotinamide/anthranilic acid (naana) cocrystal (Figure 1c) and revised the crystal structure of the salicylic acid/anthranilic acid (salana) cocrystal.

RESULTS AND DISCUSSION

Cocrystal Synthesis. Anthranilic acid is known to form three polymorphs.[47] The one we obtained commercially and used in these experiments is designated as polymorph I (ana-I) and is zwitterionic. More precisely, of the two molecules in the asymmetric unit of polymorph I, one is a "normal" non-zwitterionic molecule while the other is zwitterionic. Before studying selectivity in multicomponent reaction mixtures, we have attempted to prepare naana and nasal cocrystals separately. In the 1:1 na:ana reaction mixture, the naana forms readily and directly from reactants with no detectable intermediates. Formation of naana begins immediately upon milling, and the reaction was fully complete within 20 min milling. Crystal structure of the naana cocrystal was thus far unknown, so we have solved it from powder diffraction data (Figures 1c and S6). The crystal structure resembles that of the known nasal cocrystal[46] (Figure 1b), but it is stabilized by a larger number of hydrogen bonds since the amino group of ana acts both as an acceptor and a donor of hydrogen bonds. In the naana cocrystal, ana is not zwitterionic. The 1:1 cocrystal formation between sal and na also proceeds directly from reactants, and the reaction is complete within 20 min milling. Final product is the known nasal cocrystal.[46] Even though both reactions are complete within ca. 20 min milling, in situ monitoring revealed naana formation to be somewhat faster than nasal formation, suggesting a lower energy barrier for naana formation (Figure 2). For both cocrystal synthesis reactions, quantitative assessments based on either Raman and PXRD monitoring have revealed similar reaction profiles, indicating that the reaction mixture is crystalline and contains little or no amorphous component.

Cocrystal Selectivity and Replacement Reactions. Following cocrystal synthesis, we have attempted to predict the selectivity in formation of each cocrystal by using ab initio calculations in the solid state to estimate the relative energies of cocrystals and cocrystal coformers. Ab initio calculations are likely to provide sufficiently precise energies, which can be used to assess possibilities of cocrystal formation[48] as well as polymorphic transitions.[49] In particular, density functional theory (DFT) with newly developed functionals that include van der Waals interactions achieve good accuracy in modeling molecular crystals.[50] Of several van der Waals implementations in DFT, here we choose the nonemipirical vdW-DF-cx functional[51,52] that proved its accuracy in similar systems.[49,53,54]

Since the evaluation of (temperature dependent) Gibbs free energies from DFT comes with a very high computational cost, here we only report the relative enthalpies. It should be noted that this could be, in addition to the exchange-correlation functional, a source of imprecision in reported predictions. While comparing solids with the same composition is straightforward, cocrystals with different compositions can also be compared, provided that the overall composition is kept fixed by considering also the energy of the competing coformer (Scheme 1). Such considerations should predict which cocrystal will be stable if offered a competing coformer and which cocrystals will react to form a more stable cocrystal.

Our calculations predict all cocrystals to be more stable than pure components (Scheme 1). The naana cocrystal (see later) is only 0.5 kJ mol^{-1} more stable than the mixture of na and ana-I. The salana cocrystal is by 4.0 kJ mol^{-1} more stable than pure sal and ana-I. With 13.8 kJ mol^{-1} difference, the nasal cocrystal is most stable of all three cocrystals relative to pure components. The mixture nasal and ana-I, in the 1:1 molar ratio, is the most stable combination.[47] Therefore, sal should be able to replace ana from the naana cocrystal, while ana should not replace sal from the nasal cocrystal.

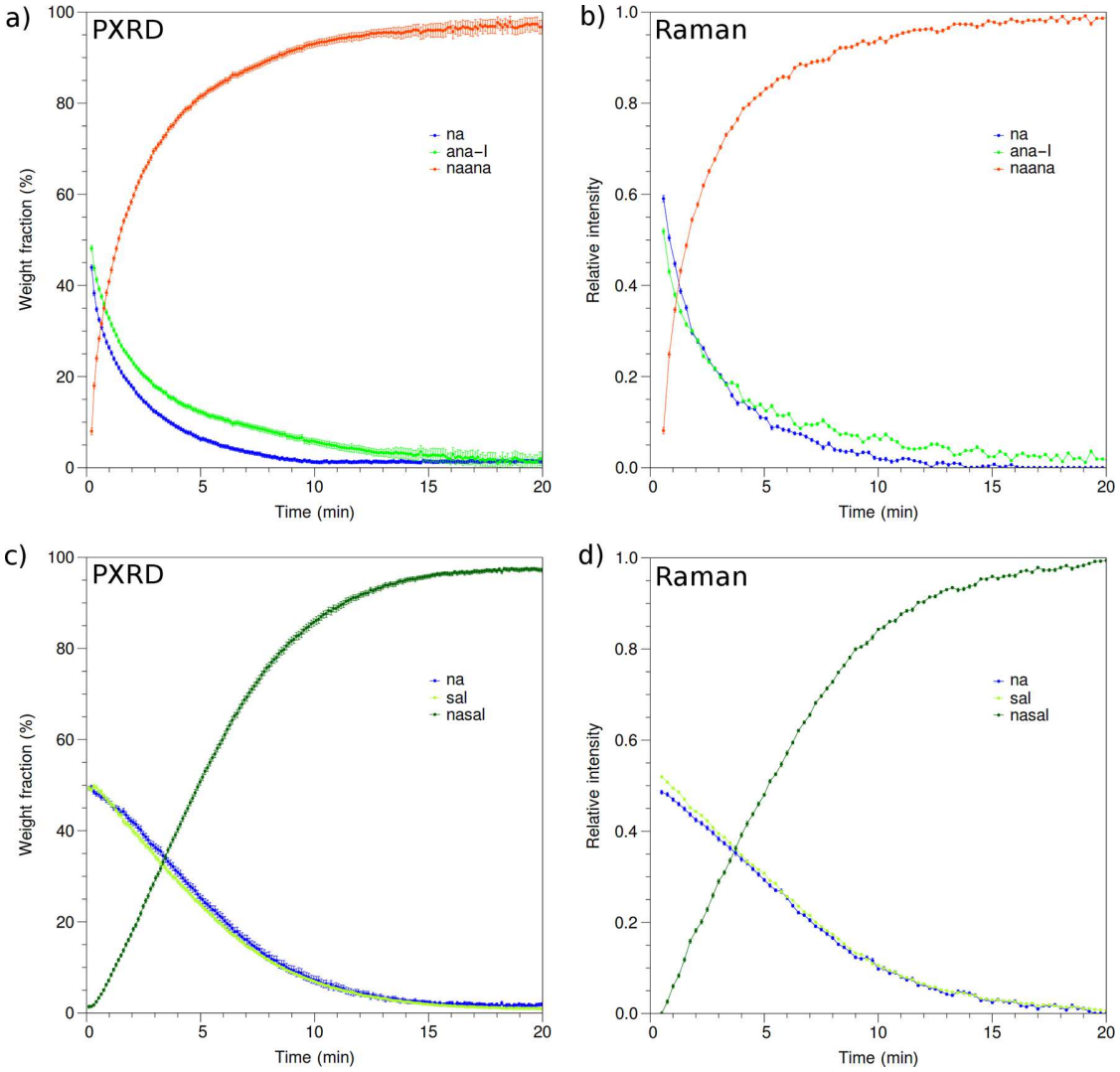

Figure 2. PXRD and Raman monitoring quantitative reaction profiles for (a, b) naana and (c, d) nasal formation.

Scheme 1. Theoretical Prediction of the Order of Stability of Cocrystals and Competing Coformers in the System of na, sal, and ana[a]

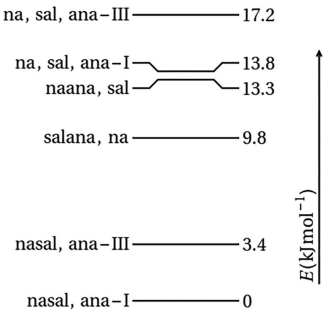

[a]Two polymorphs of ana are included, ana-I and ana polymorph III (ana-III).[47]

For replacement experiments, a competitive cocrystal coformer was added to the mechanochemically prepared naana or nasal cocrystals. Thus, we have added an equimolar amount of sal to the reaction vessel containing the naana cocrystal and, in the second experiment, an equimolar amount of ana to the mechanochemically prepared nasal cocrystal. As theory predicted, we found that ana is not able to replace sal from the nasal cocrystal, but that ana is slowly becoming amorphous during milling, evidenced by a gradual decrease in the scale factor of ana derived from Rietveld refinement (Figures S1 and S2). On the other hand, sal readily replaced ana from the naana cocrystal in a reaction mechanism that involved intermediate formation of salana (Figures 3 and S3). The replaced ana from the naana cocrystal crystallized concomitantly as a pure phase, but in a different polymorphic form than the starting ana. The in situ formed ana belongs to the monoclinic polymorph III of ana (ana-III), which no longer has zwitterionic molecules.[47] Formation of ana-III is surprising, since it was previously found to transform to ana-I upon grinding[47] and should be less stable than ana-I (Scheme 1).

Formation of ana-III provides further evidence that unusual and metastable solid species may be formed in a milled reaction environment. While a full investigation as to why the less stable polymorph ana-III was formed here is outside the scope of this work, we may offer possible explanations to its unexpected formation. Nucleation and growth of ana-III during milling may be in accordance with the Ostwald's rule of stages, but we have not observed its transformation to the stable ana-I in the period

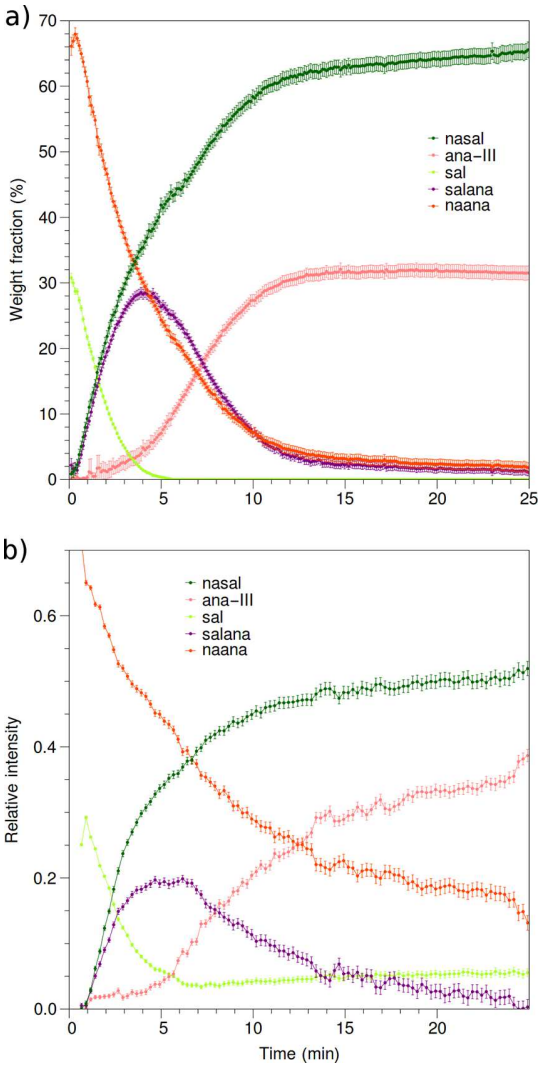

Figure 3. Reaction profiles for the mechanochemical reaction of the naana cocrystal with sal, derived from time-resolved tandem in situ monitoring by (a) PXRD and (b) Raman spectroscopy. Error bars correspond to standard deviations as obtained from the corresponding refinement procedures.

of 25 min milling. Formation of ana-III could be stochastic, as was e.g., the case with the formation of the katsenite metal–organic framework,[33] but this is impossible to judge since the experiment was repeated only once. Finally, a likely explanation for the occurrence of ana-III involves stabilization of its crystallite particles via surface interaction with the species present in the reaction mixture, as was demonstrated by Belenguer et al.[41] and by us[29] when using liquid additives.

The crystal structure of the salana cocrystal, observed here as an intermediate, was recently solved as a cocrystal of sal and ana molecules.[45] However, we have revised here the crystal structure of salana with the amino group of ana protonated in order to form three N–H···O hydrogen bonds. The protonated amino group leaves two options for the position of one hydrogen atom: either on the carboxylic group of sal or on the carboxylic group of ana. In the case of sal deprotonation, a salt would be formed, while in the case the carboxylic group of ana would be deprotonated, a zwitterionic cocrystal would form where sal would remain nonzwitterionic and ana would become zwitterionic. Since determination of hydrogen atoms from powder diffraction data may be unreliable, we have aided ourselves with ab initio calculations to rank in energy these two crystal structure candidates and found the second, zwitterionic cocrystal option, to be slightly more stable. Final Rietveld refinement was performed against high-resolution powder X-ray diffraction data, collected at the powder diffraction beamline 11-BM at the Advanced Photon Source, to reveal a chemically reasonable network of hydrogen bonds in the zwitterionic salana cocrystal (Figures 4 and S7).

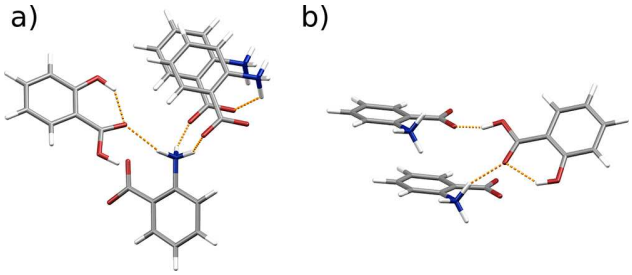

Figure 4. Hydrogen bonding in the crystal structure of the zwitterionic salana cocrystal. Hydrogen bonds are denoted with orange dashed lines. (a) Three hydrogen bonds surrounding the protonated amino group of ana and (b) the hydrogen bond between the carboxylic group of sal and the carboxylate group of ana.

With crystal structures of all participating phases now known, Rietveld refinement enabled extraction of reaction profiles which reveal immediate and concomitant formation of nasal and salana cocrystal at approximately the same rates in the beginning of the reaction, while sal is present in the reaction mixture (Figure 3). Later, formation of salana gradually slows down and stops just at the time pure sal is fully consumed when it becomes the source of salicylic acid needed for further formation of the nasal cocrystal. The crystallization of pure ana then also accelerates, but, as mentioned above, it crystallizes as polymorph III, rather than polymorph I. In situ Raman monitoring revealed essentially the same reaction course but suggests a significantly longer presence of naana and also salana, which could possibly be amorphous. Worth mentioning, in this reaction sequence, the amino group of ana underwent several proton transfers: from the starting zwitterionic ana-I, to the nonzwitterionic form in the naana cocrystal, followed again by protonation in the salana cocrystal and final crystallization of a nonzwitterionic ana-III (Scheme 2).

Competitive Experiments. Next to replacement reactions, we have performed direct competitive experiments in mixtures of na, ana-I, and sal (Figure 5). Milling equimolar amounts of na, sal, and ana-I resulted in the final formation of the nasal cocrystal. The reaction course, however, included intermediate formation of the naana cocrystal and formation of a small amount of the salana cocrystal which remained in the final reaction mixture. Rietveld analysis of the reaction course exhibits an initial decline in the weight fraction of ana-I consistent with the formation of a small amount of the naana intermediaate. As naana starts to diminish after 2 min milling, the weight fraction of ana-I increases, as the released ana crystallizes into the starting polymorph I, before it is again consumed for the formation of salana. The rate of na consumption is slightly faster than the rate of consumption of sal, consistent with parallel formation of nasal and naana. Raman monitoring revealed the same reaction mechanism with

Scheme 2. Protonation−Deprotonation Sequence of ana in the (na + ana) + sal Reaction Sequence[a]

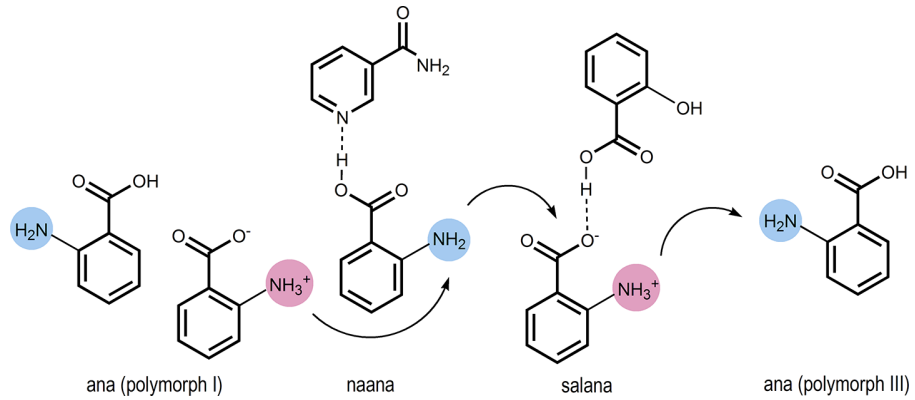

[a]Polymorph designation is given according to Etter.[47]

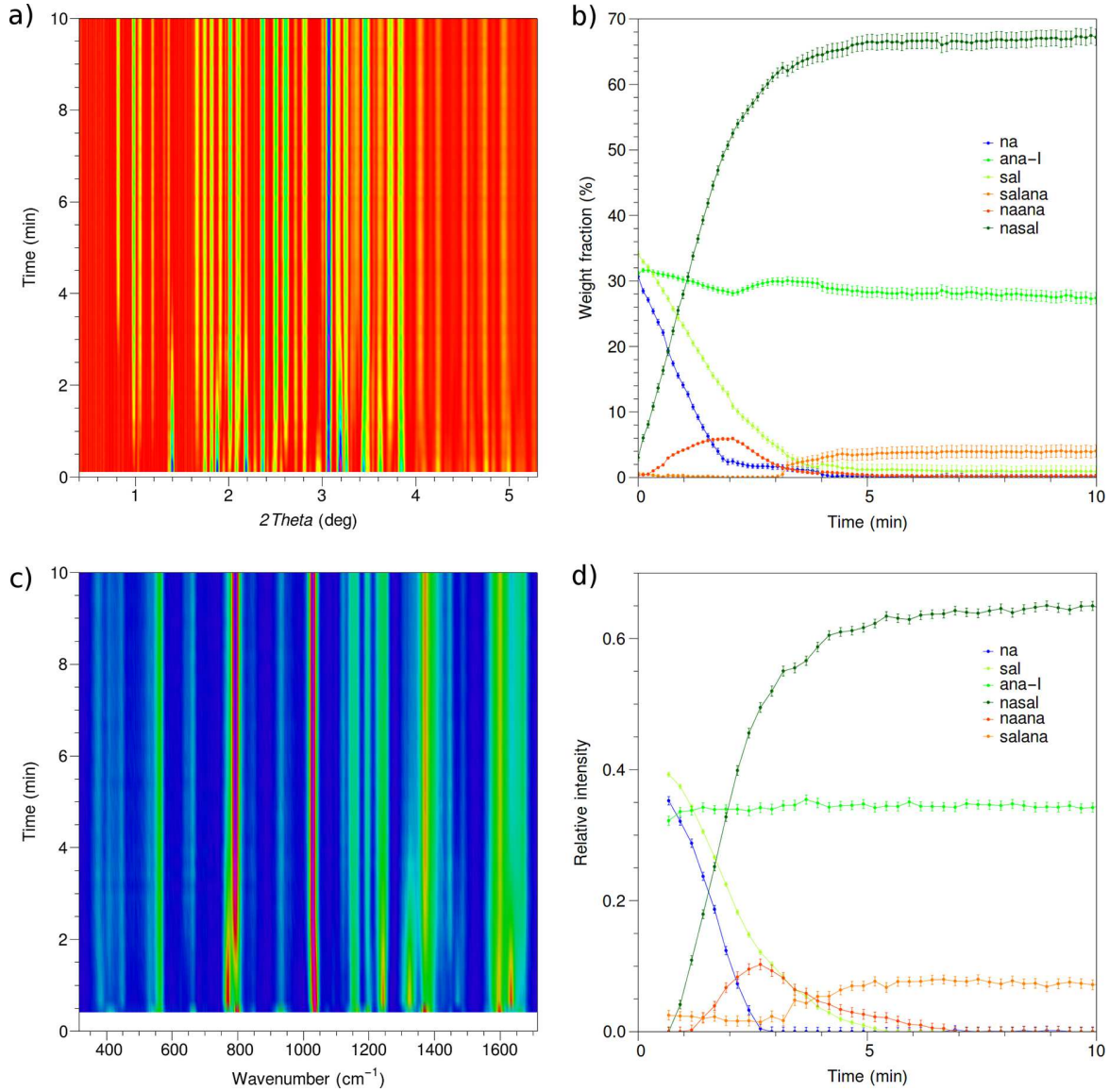

Figure 5. Competitive mechanochemical reaction of na, sal, and ana in the molar ratio 1:1:1. Tandem in situ monitoring via (a, b) PXRD and (c, d) Raman spectroscopy. (a) Two-dimensional time-resolved PXRD and (b) the corresponding reaction profile. (c) Two-dimensional time-resolved Raman spectra and (d) the corresponding reaction profile. Error bars correspond to standard deviations as obtained from the corresponding refinement procedures.

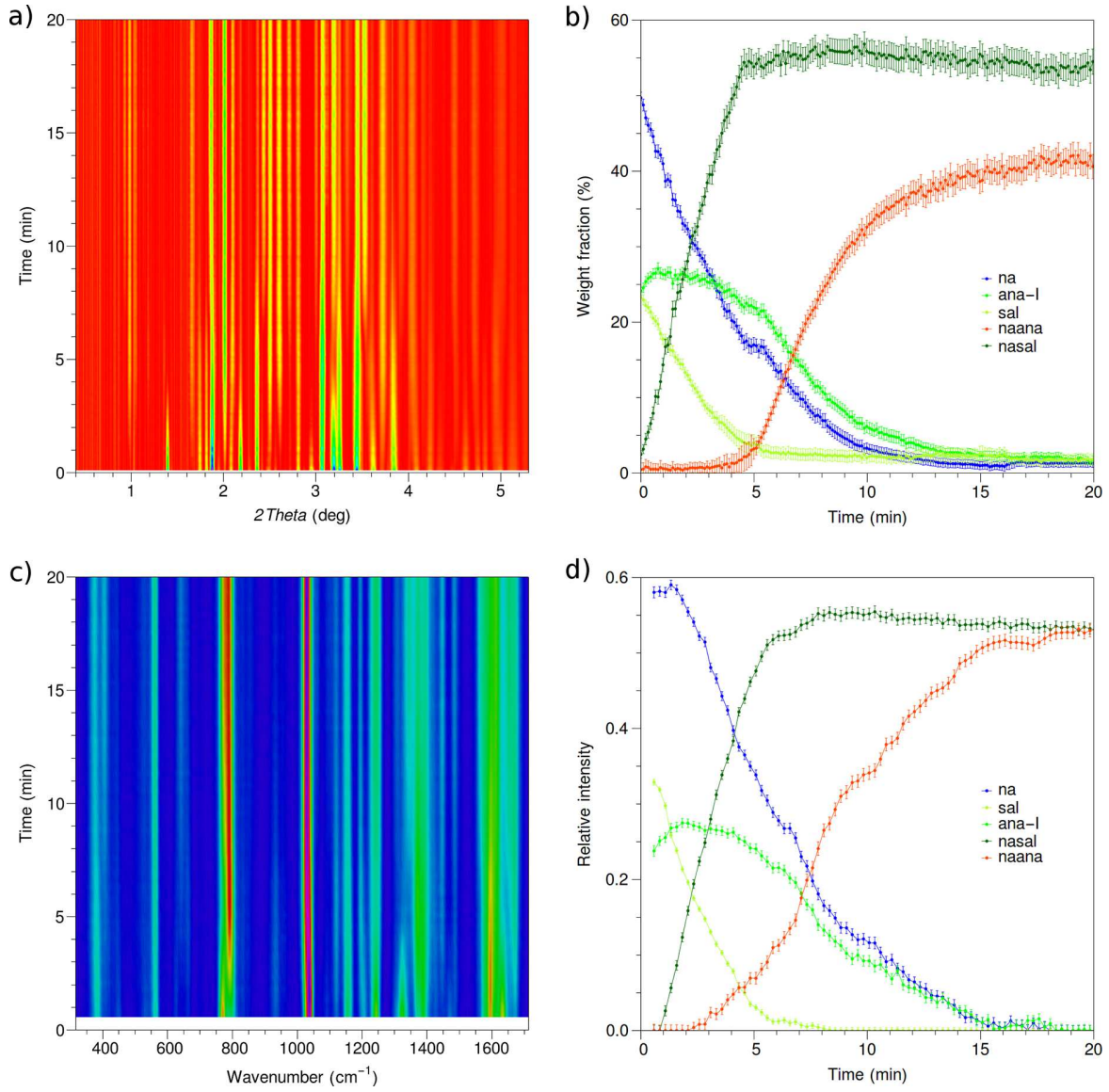

Figure 6. Competitive mechanochemical reaction of (a) na, sal, and ana in the molar ratio 1:1/2:1/2 monitored by tandem in situ (a, b) PXRD and (c, d) Raman spectroscopy. (a) Two-dimensional time-resolved PXRD and (b) the corresponding reaction profile. (c) Two-dimensional time-resolved Raman spectra and (d) the corresponding reaction profile. The reaction profiles in (b) and (d) exhibit a slight increase in the content of ana-I which is likely due to the reaction being non-homogeneous immediately after initiation of milling and thus would not correspond to an actual increase in the content of ana-I in the reaction mixture. Error bars correspond to standard deviations as obtained from the corresponding refinement procedures.

naana formation and a small amount of salana in the final mixture. Consumption of na and sal and the formation of nasal followed the same rates and trends in both PXRD and Raman monitoring indicating that nasal is highly crystalline. Formation of salana starts just after 3 min milling according to both Raman and PXRD. naana is slightly more persistent according to Raman than according to PXRD indicating the presence of amorphous or nanocrystalline naana undetectable by PXRD.

A limited study of LAG reactions was here performed where we have used methanol or propanol as liquid additives in the na:sal:ana = 1:1:1 reaction mixtures (Figures S4 and S5). Alcohols accelerated the reactions and nasal formation was finished within 5 min milling. With methanol, we observed intermediate formation of naana and the formation of a small amount of salana, which remained upon further milling. Using propanol as the liquid additive resulted in a similar reaction mechanism, but without the formation of the intermediate naana. These results strongly indicate the sensitivity of mechanochemical reactions to additives and the possibility to alter relative energies of solid species and barriers between them and thus support the concept of the energy landscape in a mechanochemical reaction environment.

Milling na, sal, and ana but now in the ratio of 1:1/2:1/2 resulted in surprisingly different reactivity as compared to the 1:1:1 mixture. The reaction mixture in this experiment contained sufficient na to fully form both nasal and naana cocrystals. Comparing PXRD and Raman monitoring (Figure 6), there are several significant similarities and differences: (i) Formation profiles of nasal are similar in PXRD and Raman monitoring, while the formation profiles of naana are

significantly different. (ii) According to PXRD monitoring, the formation of naana did not commence until crystalline sal was fully consumed and nasal formation was complete. On the other hand, Raman monitoring revealed naana formation soon after nasal started to form. (iii) Formation curve of naana derived from Raman monitoring is erratic, while it is smooth according to PXRD. (iv) On the basis of the initial stoichiometric ratio of reactants and the similarity of molecular mases of nasal and naana cocrystals, final weight fractions of nasal and naana should be similar and around 50%. However, PXRD revealed weight fraction of nasal to be around 55% and weight fraction of naana around 40% (the remaining 5% belong to minor amounts of reactants). On the other hand, Raman monitoring revealed, as expected, equal amounts of nasal and naana at the end of milling.

There are several possibilities to the observed discrepancy between in situ PXRD and Raman monitoring. It may be due to partial amorphization of naana which would result in apparent lowering of its weight fraction in Rietveld analysis, but it does not explain why naana formation is not observable by PXRD until all sal is consumed. Another possibility involves formation of a solid solution of naana in the nasal cocrystal which would increase weight fraction of nasal at the expense of naana, but this explanation assumes that naana in a solid solution in nasal would have the same Raman spectrum as pure ana, which may be an unlikely assumption. It is also likely that naana crystal growth is hindered as long as sal is present in the reaction mixture, consistent with the replacement reaction of naana with sal. Since Raman monitoring indicates presence of naana, it can only be amorphous or nanocrystalline and thus not detectable by X-ray diffraction. This is supported by a small decrease in ana weight fraction before the onset of naana crystallization. Only when sal is fully consumed, growth of microcrystalline naana can proceed when it can be detected by PXRD. This last possibility, however, does not explain the discrepancy in final weight fractions of nasal and naana.

■ CONCLUSION

We have described mechanochemical transformations and selectivity in a system of nicotinamide cocrystals with two similar aromatic carboxylic acids: salicylic acid and anthranilic acid. Cocrystals show a distinct order of selectivity and a less preferred one is readily converted to a preferred cocrystal when the competing coformer is offered. Among various approaches to explaining the order of selectivity, we find theoretical energy determination to be advantageous. With the advance in computational techniques and the availability of high-performance computers, we believe it is no longer necessary to resort to qualitative approaches, such as Etter's rules,[55,56] which in this case, would suggest opposite reactivity. Theoretical calculations will likely provide an order of stability with a high predictive power, but we should nevertheless remain aware that in milling the real sample need not conform to perfect crystals,[57,58] which are taken into theoretical predictions, but have defects, a distribution of particle sizes, and could easily contain an amorphous component.

This work has provided a clear example of different reaction profiles derived form PXRD and Raman monitoring putting an emphasis on the complementarity of the two techniques for in situ and real-time monitoring of mechanochemical reactions. While PXRD will detect bulk crystalline species, Raman monitoring, which is more sensitive to the molecular structure and the immediate molecular surroundings, will nevertheless detect a reaction occurring in an amorphous component of the reaction mixture. We therefore expect Raman monitoring to become an indispensable tool in understanding the dynamics of the mechanochemical reaction environment.

■ EXPERIMENTAL SECTION

Mechanochemical reactions were carried out as described previously[29] using a Retsch MM301 (Germany) mixer mill operating at 30 Hz. Translucent and amorphous reaction vessels made from polymethylmetacrylate (PMMA) had the internal volume of 14 mL and were purchased from InSolido Technologies (Croatia). Two halves of the vessel snapped upon closure to form a leak-proof seal. Liquids in liquid-assisted grinding reactions were added using a Gilson automated micropipet. Tandem *in situ* monitoring experiments were conducted at the ESRF beamline ID31 as described previously.[29] Briefly, the experimental hutch was air-conditioned to 20 °C, the X-ray beam and the Raman laser focus were positioned to approximately coincide on the same portion of the reaction mixture, X-ray radiation wavelength of 0.195 Å was selected using a multilayer monochromator, diffraction data were recorded on a Dectris Pilatus CdTe 2 M detector positioned 1067 mm from the sample, radial integration of the raw diffraction images was performed using PyFAI,[59] and exposure time for each pattern was 5.0 s. Time resolution between consecutive diffraction patterns was ca. 6.5 s, and time resolution of Raman spectra was typically 10 s. As milling media, two 7 mm stainless steel balls were used, each weighing 1.4 g.

Crystal structure of naana was solved from powder X-ray diffraction data collected on a laboratory Panalytical instrument in the Bragg–Brentano geometry. Structure was solved by simulated annealing in direct space using known molecular fragments of na and ana, which were treated as rigid bodies. Crystal structure solution was recognized when a meaningful hydrogen bond was assembled between molecular fragments of na and ana and with no close contacts between nonbonded atoms. The structure model was finally refined treating molecules of na and ana as rigid bodies. The crystal structure of salana was previously reported as a cocrystal of nonzwitterionic molecules of sal and ana[45] and is here revised as a zwitterionic cocrystal where the ana molecule in the cocrystal is zwitterionic. The new structure model of salana cocrystal was refined against high-resolution synchrotron powder diffraction data, collected at the 11-BM beamline of the Advanced Photon Source, using restraints on bond distances and angles as well as planarity restraints. All calculations were performed using the program Topas. Crystal structures of salana and naana are deposited with the Cambridge Crystallographic Data Center (CCDC) under deposition numbers 1581782 and 1581783 and can be retrieved from CCDC upon request.

Quantitative Rietveld refinement[60] was performed on a series of in situ collected powder diffraction patterns in an automated fashion using batch files and the command-line version of Topas, either always starting from the same input file or in a sequential manner.[26,29] Rietveld refinements included refinement of the parameters for the shifted Chebyshev polynomial used to describe the background parameters, parameters contributing the peak position and shape (contribution to the Lorenzian and Gaussian full widths at half-maximum, zero shift, unit cell parameters). No instrument contribution to peak shape was assumed. Upon convergence of Rietveld refinement for each pattern, the obtained relative crystalline phase weight fractions were output to a separate file and used for further plotting. All plots were created using the program Mathematica with the help of the SciDraw package.[61] For two-dimensional time-resolved plots, the background of each diffraction pattern was subtracted prior to plotting using the Sonneveld-Visser[62] algorithm implemented in Mathematica. Spectral range of 316–1713 cm^{-1} of Raman spectra were taken for analysis. Reaction vessel subtraction and baseline subtraction in Raman spectra was performed as previously described.[29] Raman spectra of pure phases of na, sal, ana-I, ana-III, nasal, naana, and salana were collected in the same experimental conditions. ana-III was prepared as described elsewhere.[47] Raman

reaction profiles were derived using nonnegative classic least-squares approach implemented in MATLAB.[63]

DFT calculations were performed using a plane-wave basis set code Quantum Espresso[64] with GBRV pseudopotentials[65] and vdW-DF-cx exchange-correlation functional.[51,52] The plane-wave basis set cutoff was set to 820 eV, and the first Brillouin zone was sampled by a 3 × 3 × 3 Monkhorst−Pack **k**-point mesh. In each calculation, crystal lattice and atom positions were relaxed until the change in the total energy was <0.5 meV, all the forces were smaller than 0.01 eV/Å, and pressure was <0.5 kbar.

■ ASSOCIATED CONTENT

Supporting Information

The Supporting Information is available free of charge on the ACS Publications website at DOI: 10.1021/acs.cgd.7b01512.

PXRD and Raman spectra; Rietveld fit data; crystallographic ad refinement data (PDF)

Accession Codes

CCDC 1581782−1581783 contain the supplementary crystallographic data for this paper. These data can be obtained free of charge via www.ccdc.cam.ac.uk/data_request/cif, or by emailing data_request@ccdc.cam.ac.uk, or by contacting The Cambridge Crystallographic Data Centre, 12 Union Road, Cambridge CB2 1EZ, UK; fax: +44 1223 336033.

■ AUTHOR INFORMATION

Corresponding Author

*E-mail: ivan.halasz@irb.hr.

ORCID

Tomislav Stolar: 0000-0002-9824-4462

Krunoslav Užarević: 0000-0002-7513-6485

Ivan Halasz: 0000-0002-5248-4217

Notes

The authors declare no competing financial interest.

■ ACKNOWLEDGMENTS

Financial support from the Croatian Science Foundation (Grant No. UIP-2014-09-4744) is gratefully acknowledged. I.H. is grateful to the Adris foundation for supporting this work. S.L. is supported by the Croatian Science Foundation. I.L. and P.L. are supported by the Unity Through Knowledge Fund, Contract No. 22/15 and the H2020 CSA Twinning Project No. 692194, RBI-T-WINNING. We are grateful to the team at the fine-mechanics workshop of the Ruđer Bošković Institute for their continuous support and the staff of the 11-BM beamline for powder data collection of the salana cocrystal. Use of the Advanced Photon Source at Argonne National Laboratory was supported by the U.S. Department of Energy, Office of Science, Office of Basic Energy Sciences, under Contract No. DE-AC02-06CH11357.

■ REFERENCES

(1) James, S. L.; et al. Mechanochemistry: opportunities for new and cleaner synthesis. *Chem. Soc. Rev.* **2012**, *41*, 413−447.

(2) Kaupp, G.; Schmeyers, J.; Boy, J. Waste-free solid-state syntheses with quantitative yield. *Chemosphere* **2001**, *43*, 55−61.

(3) Do, J.-L.; Friščić, T. Chemistry 2.0: Developing a New, Solvent-Free System of Chemical Synthesis Based on Mechanochemistry. *Synlett* **2017**, *28*, 2066−2092.

(4) Takacs, L. The historical development of mechanochemistry. *Chem. Soc. Rev.* **2013**, *42*, 7649−7659.

(5) Stolle, A.; Szuppa, T.; Leonhardt, S. E. S.; Ondruschka, B. Ball milling in organic synthesis: solutions and challenges. *Chem. Soc. Rev.* **2011**, *40*, 2317−2329.

(6) Kaupp, G. Organic solid-state reactions with 100% yield. *Top. Curr. Chem.* **2005**, *254*, 95−183.

(7) Wang, G.-W. Mechanochemical organic synthesis. *Chem. Soc. Rev.* **2013**, *42*, 7668−7700.

(8) Hernández, J. G.; Bolm, C. Altering Product Selectivity by Mechanochemistry. *J. Org. Chem.* **2017**, *82*, 4007−4019.

(9) Juribašić, M.; Užarević, K.; Gracin, D.; Ćurić, M. Mechanochemical C-H bond activation: rapid and regioselective double cyclopalladation monitored by in situ Raman spectroscopy. *Chem. Commun.* **2014**, *50*, 10287−10290.

(10) Hernández, J. G. C−H Bond Functionalization by Mechanochemistry. *Chem. - Eur. J.* **2017**, *23*, 17157−17165.

(11) Hermann, G. N.; Becker, P.; Bolm, C. Mechanochemical Rhodium(III)-Catalyzed C−H Bond Functionalization of Acetanilides under Solventless Conditions in a Ball Mill. *Angew. Chem., Int. Ed.* **2015**, *54*, 7414−7417.

(12) Pichon, A.; Lazuen-Garay, A.; James, S. L. Solvent-free synthesis of a microporous metal-organic framework. *CrystEngComm* **2006**, *8*, 211−214.

(13) Stolar, T.; Batzdorf, L.; Lukin, S.; Žilić, D.; Motillo, C.; Friščić, T.; Emmerling, F.; Halasz, I.; Užarević, K. In Situ Monitoring of the Mechanosynthesis of the Archetypal Metal−Organic Framework HKUST-1: Effect of Liquid Additives on the Milling Reactivity. *Inorg. Chem.* **2017**, *56*, 6599−6608.

(14) Užarević, K.; Wang, T. C.; Moon, S.-Y.; Fidelli, A. M.; Hupp, J. T.; Farha, O. K.; Friščić, T. Mechanochemical and solvent-free assembly of zirconium-based metal-organic frameworks. *Chem. Commun.* **2016**, *52*, 2133−2136.

(15) Braga, D.; Maini, L.; Grepioni, F. Mechanochemical preparation of co-crystals. *Chem. Soc. Rev.* **2013**, *42*, 7638−7648.

(16) Hasa, D.; Schneider Rauber, G.; Voinovich, D.; Jones, W. Cocrystal Formation through Mechanochemistry: from Neat and Liquid-Assisted Grinding to Polymer-Assisted Grinding. *Angew. Chem., Int. Ed.* **2015**, *54*, 7371−7375.

(17) Xu, C.; De, S.; Balu, A. M.; Ojeda, M.; Luque, R. Mechanochemical synthesis of advanced nanomaterials for catalytic applications. *Chem. Commun.* **2015**, *51*, 6698−6713.

(18) Içli, B.; Christinat, N.; Tönnemann, J.; Schuttler, C.; Scopelliti, R.; Severin, K. Synthesis of Molecular Nanostructures by Multicomponent Condensation Reactions in a Ball Mill. *J. Am. Chem. Soc.* **2009**, *131*, 3154−3155.

(19) Tan, D.; Loots, L.; Friščić, T. Towards medicinal mechanochemistry: evolution of milling from pharmaceutical solid form screening to the synthesis of active pharmaceutical ingredients (APIs). *Chem. Commun.* **2016**, *52*, 7760−7781.

(20) Bonnamour, J.; Metro, T.-X.; Martinez, J.; Lamaty, F. Environmentally benign peptide synthesis using liquid-assisted ball-milling: application to the synthesis of Leu-enkephalin. *Green Chem.* **2013**, *15*, 1116−1120.

(21) Konnert, L.; Gauliard, A.; Lamaty, F.; Martinez, J.; Colacino, E. Solventless Synthesis of N-Protected Amino Acids in a Ball Mill. *ACS Sustainable Chem. Eng.* **2013**, *1*, 1186−1191.

(22) Užarević, K.; Halasz, I.; Đilović, I.; Bregović, N.; Rubčić, M.; Matković-Čalogović, D.; Tomišić, V. Dynamic Molecular Recognition in Solid State for Separating Mixtures of Isomeric Dicarboxylic Acids. *Angew. Chem., Int. Ed.* **2013**, *52*, 5504−5508.

(23) Hernandez, J. G.; Ardila-Fierro, K. J.; Crawford, D.; James, S. L.; Bolm, C. Mechanoenzymatic peptide and amide bond formation. *Green Chem.* **2017**, *19*, 2620−2625.

(24) Pérez-Venegas, M.; Reyes-Rangel, G.; Neri, A.; Escalante, J.; Juaristi, E. Mechanochemical enzymatic resolution of N-benzylated-β^3-amino esters. *Beilstein J. Org. Chem.* **2017**, *13*, 1728−1734.

(25) Friščić, T.; Halasz, I.; Beldon, P. A.; Belenguer, A. M.; Adams, F.; Kimber, S. A. J.; Honkimäki, V.; Dinnebier, R. E. *Nat. Chem.* **2013**, *5*, 66−73.

(26) Halasz, I.; Friščić, T.; Kimber, S. A. J.; Užarević, K.; Puškarić, A.; Mottillo, C.; Julien, P.; Štrukil, V.; Honkimäki, V.; Dinnebier, R. E. Quantitative in situ and real-time monitoring of mechanochemical reactions. *Faraday Discuss.* **2014**, *170*, 203−221.
(27) Gracin, D.; Štrukil, V.; Friščić, T.; Halasz, I.; Užarević, K. Laboratory Real-Time and In Situ Monitoring of Mechanochemical Milling Reactions by Raman Spectroscopy. *Angew. Chem., Int. Ed.* **2014**, *53*, 6193−6197.
(28) Batzdorf, L.; Fischer, F.; Wilke, M.; Wenzel, K.-J. r.; Emmerling, F. Direct In Situ Investigation of Milling Reactions Using Combined X-ray Diffraction and Raman Spectroscopy. *Angew. Chem., Int. Ed.* **2015**, *54*, 1799−1802.
(29) Lukin, S.; Stolar, T.; Tireli, M.; Blanco, M. V.; Babić, D.; Friščić, T.; Užarević, K.; Halasz, I. Tandem In Situ Monitoring for Quantitative Assessment of Mechanochemical Reactions Involving Structurally Unknown Phases. *Chem. - Eur. J.* **2017**, *23*, 13941−13949.
(30) Jansen, M.; Doll, K.; Schoen, J. C. Addressing chemical diversity by employing the energy landscape concept. *Acta Crystallogr., Sect. A: Found. Crystallogr.* **2010**, *66*, 518−534.
(31) Jansen, M. The energy landscape concept and its implications for synthesis planning. *Pure Appl. Chem.* **2014**, *86*, 883−898.
(32) Andersen, J. M.; Mack, J. Decoupling the Arrhenius equation via mechanochemistry. *Chem. Sci.* **2017**, *8*, 5447−5453.
(33) Katsenis, A. D.; Puskarić, A.; Štrukil, V.; Mottillo, C.; Julien, P. A.; Užarević, M. H.; Pham, K.; Do, T. O.; Kimber, S. A. J.; Lazić, P.; Magdysyuk, O.; Dinnebier, R. E.; Halasz, I.; Friščić, T. *Nat. Commun.* **2015**, *6*, 6662.
(34) Belenguer, A. M.; Friščić, T.; Day, G. M.; Sanders, J. K. M. Solid-state dynamic combinatorial chemistry: reversibility and thermodynamic product selection in covalent mechanosynthesis. *Chem. Sci.* **2011**, *2*, 696−700.
(35) Bygrave, P. J.; Case, D. H.; Day, G. M. Is the equilibrium composition of mechanochemical reactions predictable using computational chemistry? *Faraday Discuss.* **2014**, *170*, 41−57.
(36) Belenguer, A. M.; Lampronti, G. I.; Wales, D. J.; Sanders, J. K. M. Direct Observation of Intermediates in a Thermodynamically Controlled Solid-State Dynamic Covalent Reaction. *J. Am. Chem. Soc.* **2014**, *136*, 16156−16166.
(37) Užarević, K.; Štrukil, V.; Mottillo, C.; Julien, P. A.; Puškarić, A.; Friščić, T.; Halasz, I. Exploring the Effect of Temperature on a Mechanochemical Reaction by in Situ Synchrotron Powder X-ray Diffraction. *Cryst. Growth Des.* **2016**, *16*, 2342−2347.
(38) Shan, N.; Toda, F.; Jones, W. Mechanochemistry and co-crystal formation: effect of solvent on reaction kinetics. *Chem. Commun.* **2002**, 2372−2373.
(39) Halasz, I.; Puškarić, A.; Kimber, S. A. J.; Beldon, P. J.; Belenguer, A. M.; Adams, F.; Honkimäki, V.; Dinnebier, R. E.; Patel, B.; Jones, W.; Štrukil, V.; Friščić, T. *Angew. Chem., Int. Ed.* **2013**, *52*, 11538−11541.
(40) Tireli, M.; Juribašić Kulcsar, M.; Cindro, N.; Gracin, D.; Biliškov, N.; Borovina, M.; Ćurić, M.; Halasz, I.; Užarević, K. *Chem. Commun.* **2015**, *51*, 8058−8061.
(41) Belenguer, A. M.; Lampronti, G. I.; Cruz-Cabeza, A. J.; Hunter, C. A.; Sanders, J. K. M. Solvation and surface effects on polymorph stabilities at the nanoscale. *Chem. Sci.* **2016**, *7*, 6617−6627.
(42) Etter, M. C.; Reutzel, S. M.; Choo, C. G. Self-organization of adenine and thymine in the solid state. *J. Am. Chem. Soc.* **1993**, *115*, 4411−4412.
(43) Caira, M. R.; Nassimbeni, L. R.; Wildervanck, A. F. Selective formation of hydrogen bonded cocrystals between a sulfonamide and aromatic carboxylic acids in the solid state. *J. Chem. Soc., Perkin Trans. 2* **1995**, *2*, 2213−2216.
(44) Abourahma, H.; Urban, J. M.; Morozowich, N.; Chan, B. Examining the robustness of a theophylline cocrystal during grinding with additives. *CrystEngComm* **2012**, *14*, 6163−6169.
(45) Fischer, F.; Joester, M.; Rademann, K.; Emmerling, F. Survival of the Fittest: Competitive Co-crystal Reactions in the Ball Mill. *Chem. - Eur. J.* **2015**, *21*, 14969−14974.
(46) Berry, D. J.; Seaton, C. C.; Clegg, W.; Harrington, R. W.; Coles, S. J.; Horton, P. N.; Hursthouse, M. B.; Storey, R.; Jones, W.; Friščić, T.; Blagden, N. Applying Hot-Stage Microscopy to Co-Crystal Screening: A Study of Nicotinamide with Seven Active Pharmaceutical Ingredients. *Cryst. Growth Des.* **2008**, *8*, 1697−1712.
(47) Ojala, W. H.; Etter, M. C. Polymorphism in anthranilic acid: a reexamination of the phase transitions. *J. Am. Chem. Soc.* **1992**, *114*, 10288−10293.
(48) Bučar, D.-K.; Day, G. M.; Halasz, I.; Zhang, G. G. Z.; Sander, J. R. G.; Reid, D. G.; MacGillivray, L. R.; Duer, M. J.; Jones, W. The curious case of (caffeine)·(benzoic acid): how heteronuclear seeding allowed the formation of an elusive cocrystal. *Chem. Sci.* **2013**, *4*, 4417−4425.
(49) Lončarić, I.; Popović, J.; Despoja, V.; Burazer, S.; Grgičević, I.; Popović, D.; Skoko, Ž. Reversible Thermosalient Effect of N′-2-Propylidene-4-hydroxybenzohydrazide Accompanied by an Immense Negative Compressibility: Structural and Theoretical Arguments Aiming toward the Elucidation of Jumping Phenomenon. *Cryst. Growth Des.* **2017**, *17*, 4445−4453.
(50) Reilly, A. M.; et al. Report on the sixth blind test of organic crystal structure prediction methods. *Acta Crystallogr., Sect. B: Struct. Sci., Cryst. Eng. Mater.* **2016**, *72*, 439−459.
(51) Berland, K.; Hyldgaard, P. Exchange functional that tests the robustness of the plasmon description of the van der Waals density functional. *Phys. Rev. B: Condens. Matter Mater. Phys.* **2014**, *89*, 035412.
(52) Berland, K.; Arter, C. A.; Cooper, V. R.; Lee, K.; Lundqvist, B. I.; Schroder, E.; Thonhauser, T.; Hyldgaard, P. van der Waals density functionals built upon the electron-gas tradition: Facing the challenge of competing interactions. *J. Chem. Phys.* **2014**, *140*, 18A539.
(53) Brown-Altvater, F.; Rangel, T.; Neaton, J. B. Ab initio phonon dispersion in crystalline naphthalene using van der Waals density functionals. *Phys. Rev. B: Condens. Matter Mater. Phys.* **2016**, *93*, 195206.
(54) Rangel, T.; Berland, K.; Sharifzadeh, S.; Brown-Altvater, F.; Lee, K.; Hyldgaard, P.; Kronik, L.; Neaton, J. B. Structural and excited-state properties of oligoacene crystals from first principles. *Phys. Rev. B: Condens. Matter Mater. Phys.* **2016**, *93*, 115206.
(55) Taylor, R.; Kennard, O. Hydrogen-bond geometry in organic crystals. *Acc. Chem. Res.* **1984**, *17*, 320−326.
(56) Etter, M. C. Encoding and decoding hydrogen-bond patterns of organic compounds. *Acc. Chem. Res.* **1990**, *23*, 120−126.
(57) Halasz, I. Single-Crystal-to-Single-Crystal Reactivity: Gray, Rather than Black or White. *Cryst. Growth Des.* **2010**, *10*, 2817−2823.
(58) Coquerel, G. The structural purity of molecular solids−An elusive concept? *Chem. Eng. Process.* **2006**, *45*, 857−862.
(59) Kieffer, J.; Karkoulis, D. PyFAI, a versatile library for azimuthal regrouping. *J. Phys.: Conf. Ser.* **2013**, *425*, 202012.
(60) Hill, R. J.; Howard, C. J. Quantitative phase analysis from neutron powder diffraction data using the Rietveld method. *J. Appl. Crystallogr.* **1987**, *20*, 467−474.
(61) Caprio, M. LevelScheme: A level scheme drawing and scientific figure preparation system for Mathematica. *Comput. Phys. Commun.* **2005**, *171*, 107−118.
(62) Sonneveld, E. J.; Visser, J. W. Automatic collection of powder data from photographs. *J. Appl. Crystallogr.* **1975**, *8*, 1−7.
(63) *MATLAB*, version R2016a; The MathWorks Inc.: Natick, MA, 2016.
(64) Giannozzi, P.; et al. QUANTUM ESPRESSO: a modular and open-source software project for quantum simulations of materials. *J. Phys.: Condens. Matter* **2009**, *21*, 395502.
(65) Garrity, K. F.; Bennett, J. W.; Rabe, K. M.; Vanderbilt, D. Pseudopotentials for high-throughput DFT calculations. *Comput. Mater. Sci.* **2014**, *81*, 446−452.